ChemComm

COMMUNICATION

View Article Online
View Journal | View Issue

Cite this: *Chem. Commun.*, 2025, **61**, 2095

Received 10th November 2024,
Accepted 3rd January 2025

DOI: 10.1039/d4cc05984k

rsc.li/chemcomm

Tailed molecular beacon probes: an approach for the detection of structured DNA and RNA analytes†

Brittany L. Mueller, ‡*[a] Tatiana A. Molden, ‡*[a] Jordan Hammock [a] and Dmitry M. Kolpashchikov *[abc]

Molecular beacon (MB) probes have been extensively used for nucleic acid analysis. However, MB probes fail to hybridize with folded DNA or RNA. Here, we demonstrate that MB probes equipped with extra sequences complementary to the analyte, named 'tail', can increase the signal-to-background ratio by ~40-fold and hybridization rates by ~800-fold compared to conventional MB probes. Tailed MB probes can be used as mismatched-tolerant alternatives to traditional hairpin probes for fast assays.

A molecular beacon (MB) probe is a stem-loop folded DNA structure conjugated with a fluorophore and quencher at the 5′- and 3′-end, respectively. The 15–20 nucleotide (nt) loop is complementary to the target of interest (Scheme 1A).[1,2] In a recognition event, the MB probe hybridizes with the target to form a duplex, separating the quencher and fluorophore, thus producing a 'bright' conformation.[1–4] This elegant design allows the probe to be used as a tool for various applications, including the detection of specific DNA and RNA sequences, heavy metal ions, and tumor proto-oncogenes.[5–16] Clinically significant applications of MB probe technology include the detection of *Mycobacterium tuberculosis* strains conferring rifampicin resistance and the detection of SARS-CoV-2 variants.[17,18]

However, detecting folded RNA and DNA by MB probes has posed a fundamental challenge.[2] The association between the MB probe and targets diminishes when the target is folded in a stable secondary structure (Scheme 1B).[19–24] This can impact both the thermodynamic stability of the MB probe/target complex and the hybridization rates. Improvement of MB hybridization kinetics is significant since a typical hairpin-folded probe reaches a plateau after 15–30 min of incubation in homogenous formats[4,25] and 90 min in heterogeneous formats.[26] This time extends analytical assays and reduces the practical value of MB and other harpin-shaped probes, and there is a lack of a universal and straightforward approach to increasing the hybridization rates of these probes. By exploring these hybridization rates, we can apply the discoveries to similar fields which use hairpin-shaped probes, such as DNA walker systems and multicomponent nucleic acid enzymes utilizing catalytic hairpin assays.[27,28]

Here, we report a strategy to increase both the stability of the MB/analyte complex and its hybridization rates by tailed MB probes (Scheme 1C). Tailed MB probes are equipped with a single-stranded sequence (tail) at one end that is complementary to the sequence adjacent to the MB loop-targeted sequence. The addition of the tail sequence serves a dual purpose. First,

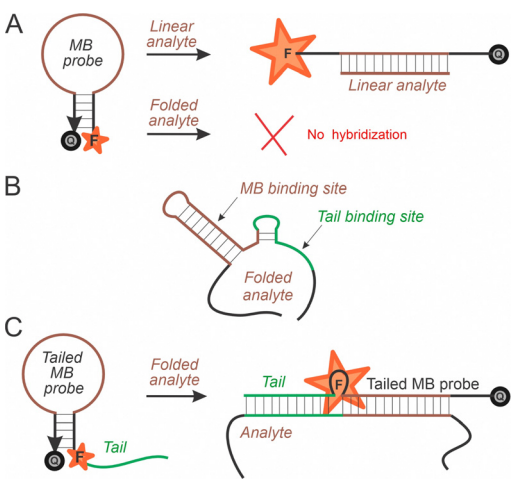

Scheme 1 The design of the tailed MB probe (see text for details). (A) Classical molecular beacon fluoresces upon binding linear analyte but cannot bind to folded DNA or RNA. (B) Nucleic acid analyte folded in secondary structure. (C) The tailed MB probe efficiently hybridizes with the folded analyte.

[a] *Chemistry Department, University of Central Florida, Orlando, Florida 32816, USA. E-mail: mueller.blynn@gmail.com*
[b] *National Center for Forensic Science University of Central Florida, Orlando, Florida 32816, USA*
[c] *Burnett School of Biomedical Sciences, University of Central Florida, Orlando, Florida 32816, USA*

† Electronic supplementary information (ESI) available. See DOI: https://doi.org/10.1039/d4cc05984k

‡ Co-First Authors.

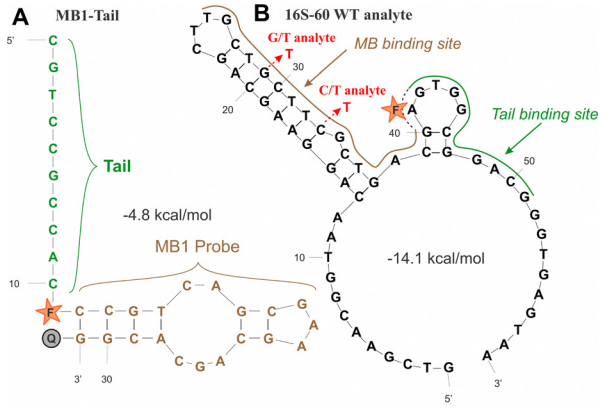

C

ΔG of analyte folding	ΔG of MB Probe/analyte	Change in ΔG upon complex formation	S/B
16S-60 WT ~ -14.1	MB1-Tail ~ -44.7	~ -25.9	42.6
	MB1 ~ -28.9	~ -10.0	1.1

ΔG are in kcal/mol

Fig. 1 Primary and secondary structures of MB1-tail probe (A) and the cognate analyte 16S-60 WT (B). Arrows indicate the two SNVs. The secondary structures and (C) Gibbs energy values (Δ*G*) were obtained at 22 °C, [MB] = 50 nM, [analyte] = 100 nM, and [Mg^{2+}] = 50 mM using Mfold.[26] The S/B was measured after an incubation period of 30 min, and the background was the MB probe with no target added.

the tail, once hybridized with the analyte, lowers the free energy of the MB/analyte complex. The lower free energy results in an equilibrium shift, which favors complex formation and increases the signal-to-background ratio (S/B). Secondly, tailed MB probes increase the hybridization rates due to the binding of the tail to secondary structure-free nucleotides, thus bringing the MB loop near the targeted sequence.

To prove our hypothesis, we chose a fragment of *E. coli* 16S rRNA that can be used to differentiate *E. coli* from other bacteria. The selected 60 nt fragment (61–120 nt of natural rRNA sequence) contained a stable stem-loop structure (Fig. 1B), also present in the natural rRNA secondary structure. An MB1 probe was designed to be complementary to one side of the stem (brown line in Fig. 1B). The lengths and sequences of the stem and the loop regions of the MB1 probe were designed based on the state-of-the-art procedure for MB probes.[2] The MB1 failed to detect the folded 60-nt DNA analog of 16S rRNA fragment as reflected by the S/B ratio of ~1.1, a phenomenon previously reported for other folded analytes.[24,29] (Fig. 1C). This S/B is too low to be useful for practical applications as the S/B should be at least 1.5 for fluorescent assays.[30]

The MB1-tail was designed by adding a 10 nt DNA 'tail' at the 5′ end of the MB1 probe (green sequence in Fig. 1A), with an internal fluorophore linked to position 5 of a thymidine. The tail sequence did not interfere with fluorophore-quencher interaction in the "closed" conformation and was complementary to the relatively accessible analyte fragment that was not folded in a stable secondary structure (as predicted by Mfold). The free energy of the MB1-tail:16S-60WT complex was reduced by 15.8 kcal mol^{-1} and resulted in a 40-fold increase in the S/B ratio compared with the MB1:16S-60WT complex (Fig. 1C and 2). Additionally, the limit of detection (LOD) for the 16S-60 WT could not be determined with MB1, but was 0.7 nM with MB1-tail (Fig. S1, ESI†), which is approximately the LOD for traditional MB probes with unfolded targets.[2]

We then assessed the effect of SNVs on hybridization thermodynamics and kinetics for the 16S analyte. We chose C/T and G/T substitutions linked to the pathogenic *E. coli* strain O157:H7.[31] We found that the MB1 probe failed to hybridize to the SNV analytes, but the MB1-tail produced a robust signal with both SNVs (Fig. S2, ESI†). This is because a single base mispairing did not result in a significant energetic penalty compared to a fully matched complex (both MB1-tail:16S-60 C/T and 16S-60 C/T complexes were destabilized only by ~2 kcal mol^{-1} in comparison with MB1-tail:16S-60 complex).

Next, we introduced mismatches into the 16S-60 analyte that did not impact the analyte's secondary structure but contained mismatches to either the stem-loop or tail of the MB1-tail probe to determine which component of the tailed MB probe was more important for hybridization to analyte (Fig. S3, ESI†). We found that a single mismatch in the region that binds to the MB loop (loop Mut 1) had a more significant impact on the initial rate and S/B than a mismatch in the tail (tail Mut 1). In contrast with the 16S-60 WT possessing a S/B of 42.6 and an initial rate of 1.59 nM s^{-1}, we found that the loop 1 Mut had a S/B of 33 and an initial rate of 0.43 nM s^{-1}, and the tail 1 Mut had a S/B of 47 and initial rate of 0.92 nM s^{-1} (Fig. S4, ESI†). When two (loop 2 Mut) or three (loop 3 Mut) mismatches were introduced into the loop-binding region, the S/B was decreased to 25 for loop 2 Mut and to 21 for loop 3 Mut, and the initial rate was reduced to ~0.20 nM s^{-1} for each. When additional mutations were introduced into the tail-binding region, the initial rates and S/B were significantly reduced to 0.03 nM s^{-1} and 24 for the tail 2 Mut, and 0.01 nM s^{-1} and 13 for the tail 3 Mut. These results suggest that, although the tailed MB probes readily hybridize with the folded analyte, they could be further optimized for selectivity by modifying the complementarity in the MB tail or stem-loop.

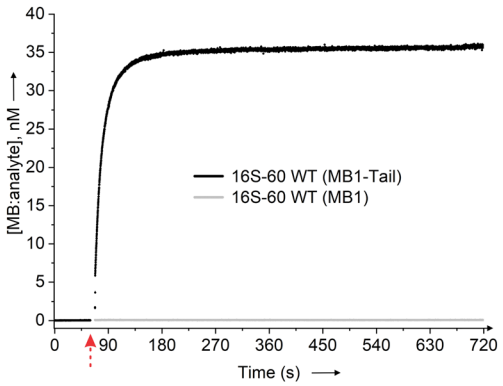

Fig. 2 Tailed MB probe improves hybridization thermodynamics. Time dependence of hybridization between 50 nM MB1 and MB1-tail with 100 nM folded 16S analyte. The hybridization buffer had [Tris–HCl] = 50 mM, [$MgCl_2$] = 50 mM, pH = 7.4, and 0.1% tween-20. The analytes were added at the 60 s time point, indicated by the red arrow, and data was collected from 70 s onward. The concentration of MB:analyte was determined *via* calibration curves with MB:analyte duplexes (Fig. S1, ESI†).

To further confirm that interaction between the tail fragment and the analyte is essential for achieving high S/B, we investigated the hybridization of MB1 and MB1-tail probes with short (16 nt) analyte fragment containing only nucleotide sequence complementary to the loop region of MB1 and MB1-tail (Fig. S5A, ESI†). We additionally tested unstructured fragments 16S-36 and 16S-27 containing complementarity to the MB probe 'tail' (Fig. S6, ESI†). The 16 nt fragment did not form a stable secondary structure ($\Delta G \sim -1$ kcal mol^{-1}, Fig. S2, ESI†). MB1 and MB1-tail produced S/B of ~5 and 7, respectively, in the presence of unfolded 16S-16 analyte (Fig. S5B, ESI†). The LOD for 16S-16 WT was 3.6 nM for MB1-tail and 6.1 nM for MB1 probe (Fig. S1, ESI†). The comparable LOD and S/B reflect similar complex stability for the two MB probes and emphasize the importance of tail fragment interaction with the folded analyte for achieving high S/B.

The hybridization rate of the MB1-tail probe was about 800-fold higher (1.6 nM s^{-1}) than the MB1 probe (0.002 nM s^{-1}, Fig. 3). At the same time, hybridization with the short 16S-16 analyte had comparable kinetics (initial rates of 0.002 nM s^{-1} and 0.007 nM s^{-1}, for MB1-tail and MB1 probe, respectively (Fig. S5, ESI†)). This result proves that the tail fragment is the key functional component of the MB1-tail probe that improves hybridization kinetics.

To check for the general applicability of our tailed MB strategy, we developed a tailed and non-tailed MB probe, τMB-tail and τMB, respectively, for the detection of another folded analyte, a fragment of tau gene and two of its mutations (Fig. S7, ESI†). The two mutations, τ-60 0C and τ-60 1A, contribute to the development of Alzheimer's disease *via* an alternative splicing pathway and skew the ratio of tau protein isoforms, leading to neurofibrillary tangles.[32] We initially designed τMB-tail and τMB as described above for the 16S-60 analyte, but the tail fragment of τMB-tail appeared to be complementary to the loop fragment (Fig. S8, ESI†). We, therefore, substituted one nucleotide in the tail region to avoid tail interference (binding to the loop region), as shown in Fig. S3 (ESI†). The τMB probe detected the folded 60-nt WT analyte with a S/B of 1.7 and LOD of 19.7 nM after 30 min, but the addition of a tail enabled τMB-tail to achieve a S/B of 5.2 and LOD of 6.5 nM (Fig. S7 and S9, ESI†). Moreover, the initial hybridization rates for τ-60 WT were determined to be ~0.030 nM s^{-1} and ~0.017 nM s^{-1} for the tailed and non-tailed MB, respectively, which reflects a two-fold improvement in hybridization rates for the tailed MB probe (Fig. S10, ESI†). Hybridization experiments with the short τ-17WT analyte revealed comparable S/B and LOD for both MB probes and somewhat slower hybridization rates for MB-tail than for the conventional MB probe (Fig. S9 and S11, ESI†), which was attributed to the ability of the τMB-tail to bind two analytes at a time. (Fig. S12, ESI†). Therefore, the design of tailed MB probes should include *in silico* analysis of such possibilities.

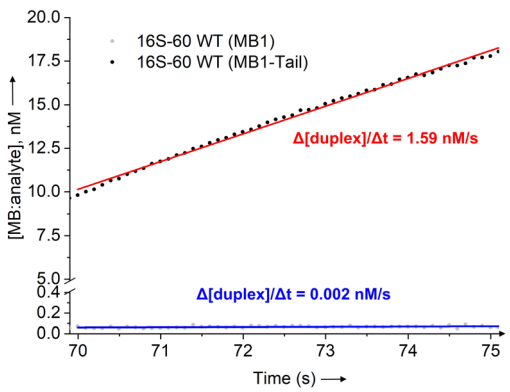

Fig. 3 MB1-tail improves hybridization kinetics. Initial hybridization rates of 16S analyte with MB1 and MB1-tail. The data was measured in triplicate, and the average was fit with a line of best fit using the concentration of the formed duplex over the first five seconds. The slope was taken to be the initial rate of duplex formation.

Next, we studied the selectivity of the tailed-MB approach. The τMB-tail probe resulted in a S/B of ~12 for the 0 C mutant and ~11 for the 1 A mutant, each representing a ~7-fold increase compared to the τMB probe (Fig. S7, ESI†). In comparison to the τMB probe, the initial rate of hybridization between the τMB-tail probe and τ-60 analytes were each determined to be ~0.1 nM s^{-1}, representing a 5- and 6-fold increase in the initial rate for the 0 C and 1 A mutants, respectively (Fig. S10, ESI†). Compared to the τ-60 WT analyte, both mutants produced a higher S/B and a faster initial rate, which can be explained by the differences in secondary structure between the WT and mutant tau analytes (Fig. S7, ESI†). Both the 0 C and 1 A mutants adopt a secondary structure with more accessible region for hybridization with the tail thus allowing the τMB-tail to hybridize more readily. Despite the 2 : 1 hybridization of the τ-60 analytes with the τMB-tail (Fig. S12, ESI†), the increase in S/B and initial rate indicates that the advantages in hybridization thermodynamics and kinetics were due to the tail fragment.

MB probes are one of the first and simplest fluorescent molecular switches available.[1,2] They have been well-studied and explored in multiple applications.[3] However, the design of MB probes is not as straightforward as it seems. The most common complications include stem invasion, stem interference, and loop interference.[2] Additionally, traditional MB probes pose a challenge in detecting folded analytes due to the high energy barrier of unfolding both the probe and the analyte.[19–24] Indeed, the MB probe stem-loop structure disfavours the analyte:MB probe-associated state and thus inhibits complex formation. Earlier, this problem was addressed by developing a universal (near ideal) MB probe in combination with additional analyte-binding arms in the context of multicomponent probes.[33,34]

The tailed MB probe studied here overcomes the challenge of detecting analytes with a stable secondary structure. We observed a ~40 and ~3 times increase in the S/B and 800- and 2-fold increases in hybridization rates for two independent systems. The latter is particularly important since hairpin probes are known to respond slowly, especially in heterogeneous assays.[25]

Tailed MB probes were not sensitive to single mismatched nucleotides. This observation agrees with the affinity selectivity dilemma, which states that hybridization probes with high affinity have low selectivity.[35] This opens the possibility of applying tailed MB probes in mutation-tolerant assays, for example, for detecting viral RNA folded in stable secondary

structures and prone to mutagenesis. Tailed MB, however, significantly reduced their responses in the presence of 2 or 3 mismatches, especially if the mismatches were complementary to the tail region of the probe, which makes them a suitable for sequence specific analysis of nucleic acids. Adopting the approach to hairpin hybridization probes used in heterogeneous formats[36,37] may significantly reduce the time for hybridization assays and make them practically useful.

MB probes equipped with additional 'tail' fragments complementary to an accessible fragment of nucleic acid analytes can improve both S/B and hybridization rates. Under room temperature, such probes are not sensitive to single nucleotide substitutions but are sensitive to double and triple nucleotide substitutions. This hairpin probe strategy is promising for reducing the time of hybridization assays. The concept of tailed MB probe can be extending to the design of other hairpin probes, which might be particularly useful for reducing the time of heterogeneous hybridization assays.

B. L. M., T. A. M., and D. M. K. conceived the experiments. B. L. M., T. A. M., and J. H. conducted the experiments. B. L. M., T. A. M., and D. M. K. wrote the manuscript. All authors provided critical feedback and helped shape the research, analysis, and manuscript. Co-first authors B. L. M. and T. A. M. contributed equally to this manuscript, and each has the right to list themselves first in author order on their CVs.

This work was supported by the National Science Foundation through the CCF: Software and Hardware Foundations under Cooperative Agreements SHF-1907824 and SHF-2226021.

Data availability

The data supporting this article have been included as part of the ESI.†

Conflicts of interest

There are no conflicts to declare.

Notes and references

1 S. Tyagi and F. R. Kramer, *Nat. Biotechnol.*, 1996, **14**, 303–308.
2 D. M. Kolpashchikov, *Scientifica*, 2012, **2012**, e928783.
3 K. Wang, Z. Tang, C. J. Yang, Y. Kim, X. Fang, W. Li, Y. Wu, C. D. Medley, Z. Cao, J. Li, P. Colon, H. Lin and W. Tan, *Angew. Chem., Int. Ed.*, 2009, **48**, 856–870.
4 A. Tsourkas, M. A. Behlke, S. D. Rose and G. Bao, *Nucleic Acids Res.*, 2003, **31**, 1319–1330.
5 S. A. Marras, *Fluoresc. Energy Transf. Nucleic Acid Probes*, 2006, 3–16.
6 Q. Huang, Z. Liu, Y. Liao, X. Chen, Y. Zhang and Q. Li, *PLoS One*, 2011, **6**, e19206.
7 S. Tyagi, *Nat. Methods*, 2009, **6**, 331–338.
8 F. Wang, G. Niu, X. Chen and F. Cao, *Eur. J. Nucl. Med. Mol. Imaging*, 2011, **38**, 1572–1579.
9 L. Wang, E.-Z. Chi, X.-H. Zhao and Q. Zhang, *Foods*, 2022, **11**, 1847.
10 H. Xu, R. Zhang, F. Li, Y. Zhou, T. Peng, X. Wang and Z. Shen, *Anal. Bioanal. Chem.*, 2016, **408**, 6181–6188.
11 H. Li, Y. Tang, W. Zhao, Z. Wu, S. Wang and R. Yu, *Anal. Chim. Acta*, 2019, **1065**, 98–106.
12 J.-E. Lee, H. Mun, S.-R. Kim, M.-G. Kim, J.-Y. Chang and W.-B. Shim, *Biosens. Bioelectron.*, 2020, **151**, 111968.
13 S. Sherrill-Mix, Y. Hwang, A. M. Roche, A. Glascock, S. R. Weiss, Y. Li, L. Haddad, P. Deraska, C. Monahan and A. Kromer, *Genome Biol.*, 2021, **22**, 1–17.
14 M. Rossetti and A. Porchetta, *Anal. Chim. Acta*, 2018, **1012**, 30–41.
15 B. Zhang, Y. Maimaiti, C. Liu, J. Li, H. Wang, H. Lin, Z. Deng, X. Lu and X. Zhang, *J. Microbiol. Methods*, 2019, **159**, 34–41.
16 D. Alexandre, A. R. Fernandes, P. V. Baptista and C. Cruz, *Talanta*, 2024, **274**, 126052.
17 D. Zahoor, S. Wani and Z. N. Wani, *Int. J. Res. Med. Sci.*, 2019, **7**, 2121.
18 P. Banada, R. Green, S. Banik, A. Chopoorian, D. Streck, R. Jones, S. Chakravorty and D. Alland, *J. Clin. Microbiol.*, 2021, **59**, e00845-21.
19 J. F. Hopkins and S. A. Woodson, *Nucleic Acids Res.*, 2005, **33**, 5763–5770.
20 B. A. Armitage, *Drug Discovery Today*, 2003, **8**, 222–228.
21 S. A. Kushon, J. P. Jordan, J. L. Seifert, H. Nielsen, P. E. Nielsen and B. A. Armitage, *J. Am. Chem. Soc.*, 2001, **123**, 10805–10813.
22 S. Lane, J. Evermann, F. Loge and D. R. Call, *Biosens. Bioelectron.*, 2004, **20**, 728–735.
23 W.-T. Liu, H. Guo and J.-H. Wu, *Appl. Environ. Microbiol.*, 2007, **73**, 73–82.
24 J. Grimes, Y. V. Gerasimova and D. M. Kolpashchikov, *Angew. Chem., Int. Ed.*, 2010, **49**, 8950–8953.
25 C. Fan, K. W. Plaxco and A. J. Heeger, *Proc. Natl. Acad. Sci. U. S. A.*, 2003, **100**, 9134–9137.
26 M. Zuker, *Nucleic Acids Res.*, 2003, **31**, 3406–3415.
27 Y. Yang, F. Wang, J. Li, S. He, Y. Lyu, H. Yang, R. Cai and W. Tan, *Anal. Chem.*, 2023, **95**, 15042–15048.
28 H. Yan, G. Cao, J. Wang, X. Zhu, S. Dong, Y. Huang, M. Chao, Y. Li, F. Gao and L. Hua, *Biosens. Bioelectron.*, 2024, **256**, 116278.
29 C. Nguyen, J. Grimes, Y. V. Gerasimova and D. M. Kolpashchikov, *Chemistry*, 2011, **17**, 13052–13058.
30 M. Stancescu, T. A. Fedotova, J. Hooyberghs, A. Balaeff and D. M. Kolpashchikov, *J. Am. Chem. Soc.*, 2016, **138**, 13465–13468.
31 W. A. Ferens and C. J. Hovde, *Foodborne Pathog. Dis.*, 2011, **8**, 465–487.
32 T. Guo, W. Noble and D. P. Hanger, *Acta Neuropathol.*, 2017, **133**, 665–704.
33 D. M. Kolpashchikov, *Acc. Chem. Res.*, 2019, **52**, 1949–1956.
34 B. L. Mueller, M. J. Liberman and D. M. Kolpashchikov, *Nanoscale*, 2023, **15**, 5735–5742.
35 V. V. Demidov and M. D. Frank-Kamenetskii, *Trends Biochem. Sci.*, 2004, **29**, 62–71.
36 A. Abi and E. E. Ferapontova, *Anal. Bioanal. Chem.*, 2013, **405**, 3693–3703.
37 J. Huang, X. Yang, X. He, K. Wang, J. Liu, H. Shi, Q. Wang, Q. Guo and D. He, *TrAC, Trends Anal. Chem.*, 2014, **53**, 11–20.

